



Influence of oxidizing gas atmosphere on thermal stability and safety risk of 1-butyl-3-methylimidazolium tetrafluoroborate

Rui Xia¹ · Shang-Hao Liu² · Wen-Tao Wang¹ · Feng-Jen Chu³

Received: 29 June 2022 / Accepted: 21 October 2022 / Published online: 11 November 2022
© Akadémiai Kiadó, Budapest, Hungary 2022, corrected publication 2022

Abstract

1-Butyl-3-methylimidazolium tetrafluoroborate ([Bmim]BF₄) is often used as an extractive desulfurization of liquid fuels. However, the role of air and nitrogen atmospheres on thermal effect of [Bmim]BF₄ has been shown to the opposite. Thus, the effect of oxidizing gases on thermal stability and safety risk of [Bmim]BF₄ is worth further investigation. In this study, the thermal stability, decomposition mechanism, and thermal hazards of [Bmim]BF₄ were studied by thermogravimetric (TG), simultaneous application of thermogravimetric with a Fourier transform infrared spectroscopy (TG-FTIR), and accelerated adiabatic calorimetry (ARC). Obtained by thermogravimetric experiments, the long-term thermal stability of [Bmim]BF₄ is MOT₈₀₀₀=92 °C under air and MOT₈₀₀₀=112 °C under nitrogen. TG-FTIR shows that the decomposition mechanism is different in the two atmospheres; CO₂ is only produced under air, indicating that the decomposition products of [Bmim]BF₄ undergo combustion and release huge heat, which explains the exotherm of DSC images in air. In adiabatic experiments, different atmospheres affect the decomposition reaction order of [Bmim]BF₄. Nitrogen suppresses the thermal effect of [Bmim]BF₄, because although the decomposition rate of [Bmim]BF₄ before runaway is much greater under nitrogen than under air, the maximum temperature and maximum pressure are still less than under air. The thermal stability, thermal effect, and adiabatic runaway of [Bmim]BF₄ in different atmosphere are a typical representations of ILs, which proves that oxidizing atmosphere has a great negative influence on thermal hazards of [Bmim]BF₄.

Keywords 1-Butyl-3-methylimidazolium tetrafluoroborate · Thermal stability · Decomposition mechanism · Adiabatic runaway

List of symbols

A	Frequency factor (s ⁻¹)
k	Arrhenius rate constant
E_a	Apparent activation energy (kJ mol ⁻¹)
α	Conversion degree
β	Heating rate (°C min ⁻¹)
T	Temperature (°C)
T_0	Initial temperature (°C)
T_{end}	Terminal decomposition temperature (°C)

T_p	Peak decomposition temperature (°C)
T_{onset}	Onset decomposition temperature (°C)
ΔT_{ad}	Adiabatic temperature rise (°C)
T_f	Ending temperatures (°C)
MOT	Maximum operation temperature (°C)
MOT ₈₀₀₀	8000 Hours maximum operating temperature
MOT ₂₄	24 Hours maximum operating temperature
MOT ₁	1 Hour maximum operating temperature
R	Universal gas constant (J mol ⁻¹ K ⁻¹)
m_T	Self-heating rate (°C min ⁻¹)
n	Reaction order
P_{max}	Maximum pressure (bar)
T_{max}	Maximum temperature (°C)
m	Mass of sample (kg)
φ	Inertia factor
T_{end}	End temperature (°C)
T_{star}	Start temperature (°C)
M_c	Mass of ARC bomb (g)
M_s	The mass of the samples (g)

✉ Shang-Hao Liu
shliu998@163.com

✉ Feng-Jen Chu
fjenchu@163.com

¹ School of Chemical Engineering, AUST, Huainan 232001, Anhui, China

² Department of Chemical and Materials Engineering, National Yunlin University Science and Technology, 123, University Rd. Sec. 3, 64002, Douliou, Yunlin, Taiwan

³ School of Medicine, AUST, Huainan 232001, Anhui, China

C_{vc}	The heat capacity of the bomb $J g^{-1} K^{-1}$
C_{vs}	The heat capacity of the samples $J g^{-1} K^{-1}$

Introduction

Ionic liquid (ILs) composed of organic cations and inorganic or organic anions as liquid state around 25 °C is known as room temperature molten salts [1, 2]. Compared with traditional organic solvents, ILs exhibit a series of excellent properties, such as extremely low volatility, high stability, and wide electrochemical window [3, 4]. A large amount of literature shows that ILs have promising applications as green low temperature electrolytes in metal electrodeposition, preparation of energy-containing materials, and other related fields [5]. According to market research, the global ILs market is on the rise and is expected to reach a total of more than US \$60 million by 2025 [6, 7]. Recognizing the thermal safety of ILs themselves is of great significance for safe production. Most of the literature focuses more on the application of ILs, but ignores the thermal safety of ILs during production and application [8]. The traditional method of judging the safety of ILs is based on flash point, which obviously has drawbacks. For instance, ILs have low volatility and are obviously difficult to form combustion mixtures with air [9]. Therefore, ILs are always considered noncombustible; the use of traditional methods to judge the safety of ILs is extremely dangerous. Most of the combustion of ILs is related to the positive heat generated, the oxygen content, and the decomposition products [9]. The minimum temperature at which ILs can be used is limited by their melting point, and the thermal stability limits the maximum temperature [10]. The thermal stability of ILs is often determined by a thermogravimetric analyzer (TG) with a constant rate of temperature rise under different atmospheres [11]. The temperature rise rate chosen for this paper is 1.0, 2.0, 4.0, and 10.0 °C min⁻¹. The temperature corresponding to the mass loss (1%) is called the onset temperature (T_{onset}) and is often used as a synonym for the decomposition temperature to define the thermal stability of ILs [12]. However, studies indicated that ILs decompose at a temperature prominently lower than T_{onset} , which is caused by a high heating rate of 10.0 °C min⁻¹ with the initial thermal degradation temperature being quickly exceeded [13]. Usually the onset temperature is used as a reference temperature, which can lead to an overestimation of the upper operating temperature [14–16]. Therefore, more thermal analysis technical methods are needed to fully evaluate the ILs properties.

1-Butyl-3-methylimidazolium tetrafluoroborate ([Bmim]BF₄) is a potential desulfurization reagent of liquid fuels [17]. The combustion of liquid fuels is very violent and releases a lot of heat, if thermal stability and thermal hazards of [Bmim]BF₄ are not sufficiently understood, which may

also cause great hazards. Because of its own non-toxic and non-corrosive, low vapor pressure and other excellent properties, [Bmim]BF₄ acts as an extractant to replace the traditional organic extractant in azeotropic distillation. [Bmim]BF₄ as an extractant needs to extract azeotropes in a high temperature environment, and how its own properties change is crucial to the extraction effect [18]. So in-depth study of the thermal stability and thermal hazards of [Bmim]BF₄ is needed. During the visualization experiment, [Bmim]BF₄ has obvious spattering in two atmospheres at high temperatures; this indicates that [Bmim]BF₄ decomposition by heat will produce a large amount of gas, for which the type of gas, release rate, and volume of release will have an impact on safety, if in a confined space it may cause combustion or even explosion. From the paper by Wang et al., it was found that [Bmim]BF₄ has opposite thermal effects in two atmospheres [19]. There is only one exothermic peak and [Bmim]BF₄ emits a total of 2629 J g⁻¹ under air, which was almost 5.25 times higher than the limitation of 500 J g⁻¹ formulated by European Classification, so it is very necessary to analyze the thermal properties of [Bmim]BF₄ in air, while in the conditions of nitrogen there is only a small exothermic peak but a huge heat absorption peak with a total absorption of 1315 J g⁻¹ [19]. Different decomposition mechanisms cause different thermal effects under the two gases, which need to be further analyzed by more thermal analysis methods. The methods employed were as follows:

- (1) To obtain the thermal stability of [Bmim]BF₄, thermogravimetric analyzer (TG) was used under different atmospheres conditions.
- (2) To describe the thermal decomposition mechanisms of [Bmim]BF₄ under different atmospheres, thermogravimetry coupled with Fourier transform infrared spectroscopy (TG-FTIR) was applied.
- (3) To estimate the parameters of process safety during a thermal runaway reaction, accelerating rate calorimeter (ARC) was used under adiabatic conditions.

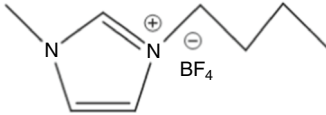
The above experiments were repeated three times for each group to eliminate experimental uncertainties and to ensure the accuracy of the experimental data. Through a comprehensive and in-depth analysis of [Bmim]BF₄, we are able to fully understand this substance and improve its safety in production, use, and transportation.

Experimental details

Sample

1-Butyl-3-methylimidazolium tetrafluoroborate ([Bmim]BF₄) is a colorless and transparent liquid and was purchased

Table 1 Basic parameters of [Bmim]BF₄

Property	Data	Molecular structure
Formula	C ₈ H ₁₅ N ₂ BF ₄	
Molecular mass	226.02	
Density	1.26 g cm ⁻³	
Appearance	Transparent	
Purity	99%	

from Hua Wei Rui Ke Chemical Corp. Beijing, China. Store sealed at room temperature prior to experimentation. The chemical properties of the substances are shown in Table 1.

Experimental equipment

Thermogravimetric analyzer (TGA)

TGA 2 (Mettler Toledo, Switzerland) is commonly conducted to examine the relationship between quality and temperature by setting temperature conditions through meter programs. The initial exothermic reaction temperature, peak temperature, final reaction temperature, and maximum mass loss derivative were detected using the TGA thermal analysis system. It was used to study the thermal stability of [Bmim]BF₄. The samples were loaded into a 70- μ L capped alumina crucible, and the mass of each sample was controlled at 2.0 ± 0.1 mg. In the atmosphere of nitrogen and air, the purge rate was controlled at 20 mL min^{-1} . Since the corrected β value for the TGA instrument in the study was $4.0 \text{ }^\circ\text{C min}^{-1}$, the heating rates are, respectively, 1.0, 2.0, 4.0, $10.0 \text{ }^\circ\text{C min}^{-1}$. The β value is chosen strictly in accordance with the recommendation that the ratio of the maximum β value ($10.0 \text{ }^\circ\text{C min}^{-1}$) to the minimum β value ($1.0 \text{ }^\circ\text{C min}^{-1}$) is not less than 5 [20, 21]; the temperature range of the experiment is controlled at $30\text{--}700 \text{ }^\circ\text{C}$. Because the substance has a spattering phenomenon, a lid with a small hole is added to the crucible to protect the apparatus during thermogravimetric experiments [22, 23].

Combustion mechanism analysis via thermogravimetry with Fourier transform infrared spectroscopy (TG-FTIR)

A TGA 2 (Mettler Toledo, Switzerland) coupled with an FTIR spectrometer iS20 (Thermo Fisher, USA) was used to analysis of pyrolysis products of [Bmim]BF₄ under nitrogen and air by combined thermogravimetric experiments and Fourier transform infrared spectroscopy. Maintain the same experimental conditions for both sets of experiments except

for different atmospheric conditions. For temperature control in thermogravimetric experiments at $30\text{--}500 \text{ }^\circ\text{C}$, the heating rate is $10 \text{ }^\circ\text{C min}^{-1}$. From the previous thermogravimetric experiments, it is known that because the crucible was covered, the amount of substance was increased in order to detect the pyrolysis products of the substance smoothly, and 5 ± 0.1 mg was added to the alumina crucible with a lid, and the gas purge rate was 20 mL min^{-1} ; the FTIR spectra were analyzed at a 4 cm^{-1} resolution with 8 scans in the range of $4000\text{--}700 \text{ cm}^{-1}$ [24].

Accelerating rate calorimeter (ARC)

Accelerating rate calorimeter (ARC) from Thermal Hazard Technology (THT), Inc. (Bletchley, England) was used to measure the thermal hazard potential of [Bmim]BF₄ under adiabatic conditions. Add 2 ± 0.1 g sample to the samples bomb of stainless steel; the mass of bomb is 16.2 g. The temperature range of the experiment under air condition is $260\text{--}550 \text{ }^\circ\text{C}$. The temperature range is set to $300\text{--}550 \text{ }^\circ\text{C}$ in nitrogen, in order to maintain nitrogen conditions inside the ARC bomb; the loaded ARC bomb needs to be placed in a nitrogen-filled glove box for a period of time. The sensitivity of both experiments is 0.2 min^{-1} , waiting time is 15 min, and temperature step is $5.0 \text{ }^\circ\text{C}$ [25, 26].

Result and discussion

Thermal stability assessment

Thermogravimetric experiments were used to evaluate the thermal stability of [Bmim]BF₄ under nitrogen or air. The corresponding TG and DTG curves are shown in Figs. 1 and 2. There is only one mass loss phase in both atmospheric

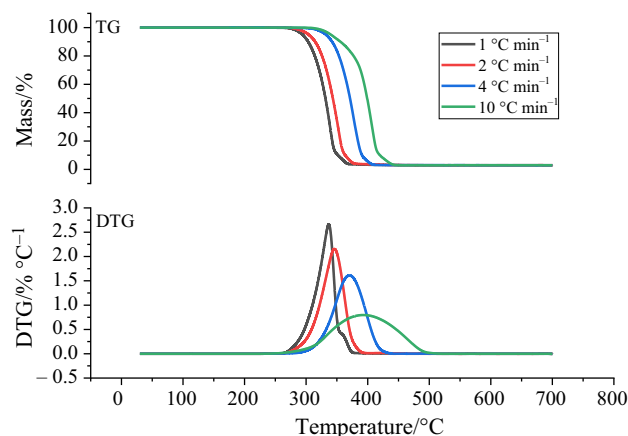


Fig. 1 TG and DTG curves of [Bmim]BF₄ at different heating rates in nitrogen atmosphere

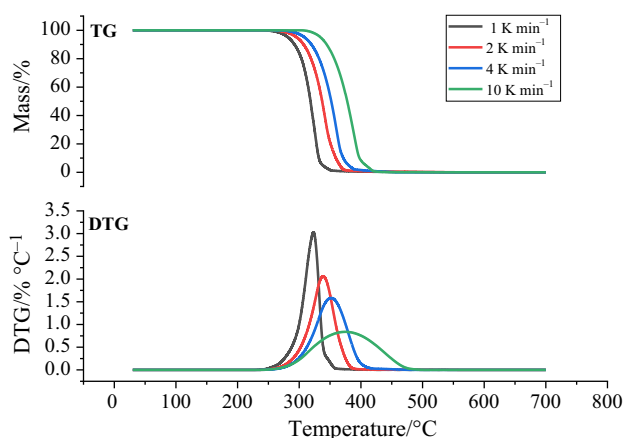


Fig. 2 TG and DTG curves of [Bmim]BF₄ at different heating rates in air atmosphere

conditions. Under air, [Bmim]BF₄ will be completely pyrolyzed. In contrast, [Bmim]BF₄ will not be completely pyrolyzed and there will be 2.9% remaining under nitrogen, because the organic matter in the ILs cannot be decomposed by oxidation. As shown in Tables 1 and 2, the decomposition temperature under nitrogen is higher than that under air, which proves that [Bmim]BF₄ is more stable under nitrogen. The mass loss rate in air is different from that in nitrogen atmosphere, indicating different mechanisms of thermal decomposition in air or nitrogen [27]. The decomposition temperature of [Bmim]BF₄ in both atmospheres increased with increasing heating rate. This trend could be comprehended by the fact that the rate of thermal degradation was determined by both the thermodynamics and thermokinetics of the decomposition process [28].

Calculation method of thermodynamic parameters

The apparent activation energy (E_a) can be used to indicate the minimum amount of energy required for a chemical reaction to occur, so the higher the E_a , the more difficult the reaction will be. Model-free methods allow evaluation of kinetic parameters without pre-selection of reaction models, the Flynn–Wall–Ozawa (FWO) method is one of the most commonly used methods, and its calculation

is relatively simple and applicable to linear heating rate conditions, but its accuracy is poor. The addition of the Kissinger–Akahira–Sunose (KAS) method can improve the accuracy of the E_a calculation and can verify the calculation results with each other. As two integral isotransformation methods, the FWO method is obtained by a very coarse Doyle approximation, while the coarse temperature approximation of the integral leads to E_a inaccuracy, and the KAS method is obtained by a more precise approximation of the temperature integral type parameter. Compared to the FWO method, the KAS method offers a significant improvement in the accuracy of the E_a values. The FWO and KAS are used to calculate thermodynamic parameters in the paper [29–31].

The kinetics is expressed by applying the following equation.

$$\frac{d\alpha}{dt} = k(T) \times f(\alpha) \quad (1)$$

where da/dt is the conversion rate, $k(T)$ is the Arrhenius rate constant, and $f(\alpha)$ is the differential mechanism function.

Among them, the rate constant-temperature relation proposed by Arrhenius by simulating the equilibrium constant-temperature relation is the most general.

$$k(T) = A \exp\left(-\frac{E}{RT}\right) \quad (2)$$

where A is the frequency factor and R is the universal gas constant.

Combining Eqs. (1) and (2), according to the Arrhenius equation, and considering the impact of the heating rate.

$$\beta = \frac{dT}{dt} \quad (3)$$

where T , t , and β represent temperature, time, and heating rate, respectively. Equation (1) is rearranged in the following form of Eq. (4).

$$\frac{d\alpha}{dT} = \frac{A}{\beta} \times \exp\left(-\frac{E_a}{RT}\right) \times f(\alpha) \quad (4)$$

FWO and FAS can be represented by Eqs. (5) and (6), respectively [32, 33].

Table 2 Decomposition feature parameters of [Bmim]BF₄ are obtained by TGA in nitrogen atmosphere

$\beta/^\circ\text{C min}^{-1}$	$T_{\text{onset}}/^\circ\text{C}$	$T_{\text{pl}}/^\circ\text{C}$	$T_{\text{end}}/^\circ\text{C}$
1	298.6	337.0	363.8
2	320.7	345.0	364.9
4	347.0	369.9	392.0
10	374.2	393.2	423.1

Table 3 Decomposition feature parameters of [Bmim]BF₄ are obtained by TGA in air atmosphere

$\beta/^\circ\text{C min}^{-1}$	$T_{\text{onset}}/^\circ\text{C}$	$T_{\text{pl}}/^\circ\text{C}$	$T_{\text{end}}/^\circ\text{C}$
1 °C min ⁻¹	286.2	375.1	350.0
2 °C min ⁻¹	314.9	354.3	359.1
4 °C min ⁻¹	329.2	338.8	373.4
10 °C min ⁻¹	346.9	323.4	408.7

$$\ln\beta = \ln\left(\frac{0.0048AE_a}{R}\right) - 1.052\frac{E_a}{RT} \tag{5}$$

$$\ln\left(\frac{\beta}{T^2}\right) = \ln\left(\frac{AR}{E_aG(\alpha)}\right) - \frac{E_a}{RT} \tag{6}$$

To calculate E_a , a total of sixteen sets of conversion rates (α) from 5 to 80% were taken separately. Use both FWO and KAS methods to make scatter plots of $\ln\beta$, $1000/T$ versus $\ln(\frac{\beta}{T^2})$, $1000/T$, respectively, and to perform a linear fit to the resulting images. The results show that the two methods have a good linear relationship ($R^2 > 0.96$), as shown in Figs. 3 and 4. In Fig. 5, a clear relationship between E_a and α is shown, the average activation energy in air is 100 kJ mol^{-1} , and the average activation energy obtained under nitrogen is 115 kJ mol^{-1} . The conversion rate is

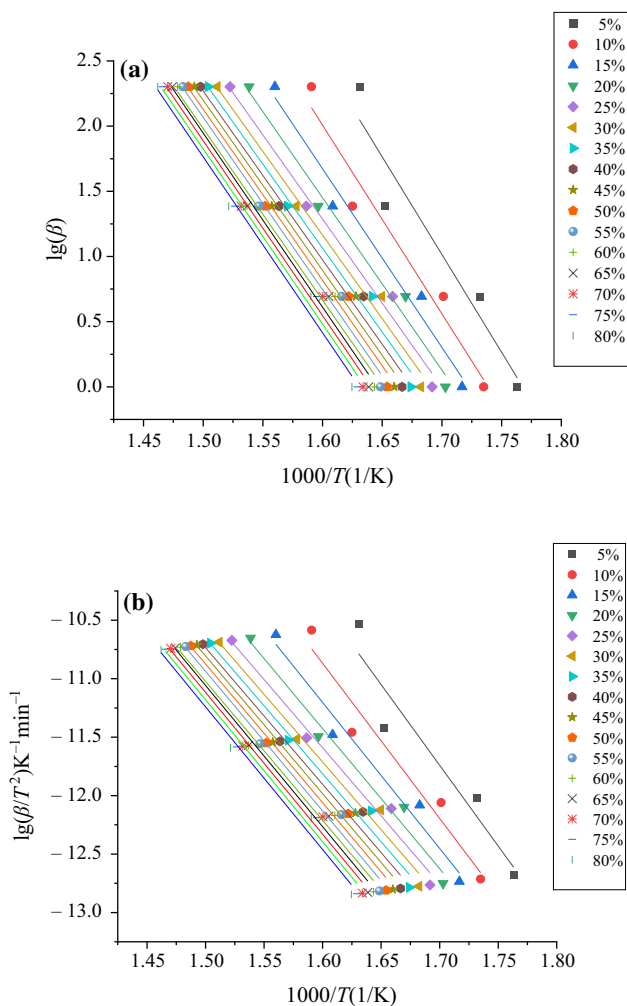


Fig. 3 Linear curves for a $\ln(\beta)$ versus $1000/T$ by the FWO method and b $\ln(\beta/T^2)$ versus $1000/T$ by the KAS method in nitrogen atmosphere

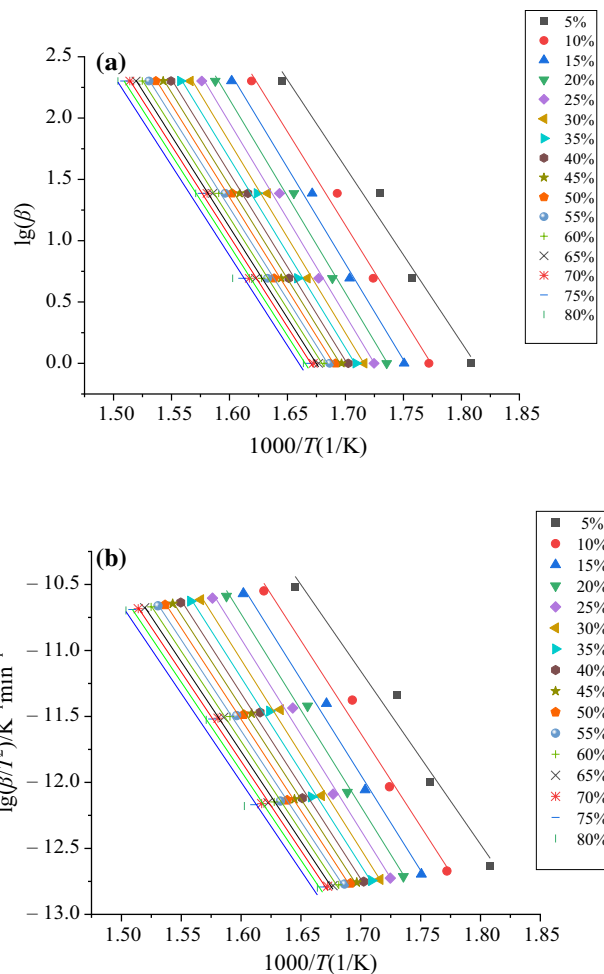


Fig. 4 Linear curves for a $\ln(\beta)$ versus $1000/T$ by the FWO method and b $\ln(\beta/T^2)$ versus $1000/T$ by the KAS method in air atmosphere

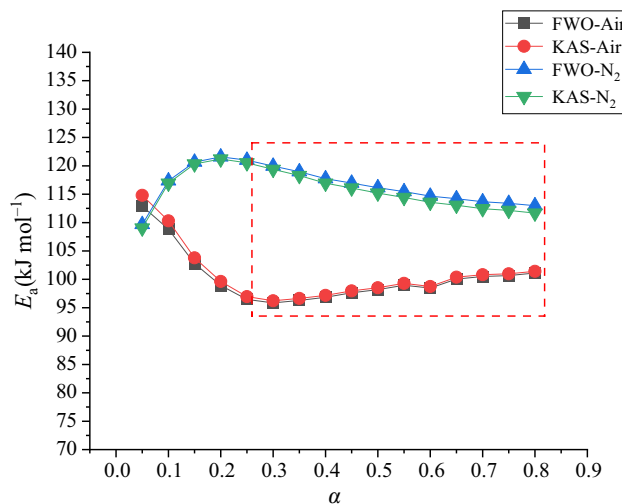


Fig. 5 Activation energy of thermal decomposition of $[Bmim]BF_4$ in two atmospheres depends on the conversion rate

Table 4 Kinetic parameters E_a and K_0 for the decomposition processes and calculated maximum operation temperature (MOT) of [Bmim]BF₄

	E_a /kJ/mol	K_0 /min ⁻¹	MOT ₈₀₀₀ /°C	MT ₂₄ /°C	MOT ₁ /°C
Nitrogen	117	1.5×10^8	112	185	238
Air	102	8.4×10^6	92	169	225

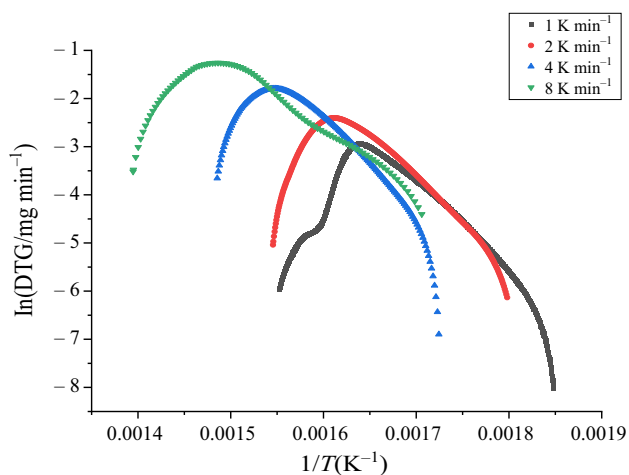


Fig. 6 $\ln(\text{DTG})$ versus $1/T$ of [Bmim]BF₄

influenced by the chosen baseline and equipment noise in the beginning of the phase [34]. Therefore, the activation energy in the range of 0.3 to 0.8 is considered reliable for the conversion rate. Obviously, the value of E_a is always close to the average E_a for different α fluctuations. Vyazovkin et al. found that E_a does not vary greatly in the range of α and there is no peak in the reaction rate curve; then, the process is dominated by the single-step model [35].

Long-term thermal stability

The kinetic parameters obtained from the short-term dynamic thermogravimetric experiment can also be used in long-term thermal stability calculation. (The corresponding residual mass is about 99%.) The thermal stability is not well judged based only on the temperature parameters obtained from thermogravimetric analysis. Based on the evaporation and pyrolysis kinetic model of ILs, maximum operating temperature (MOT) can be obtained, which can be used to characterize the long-term thermal stability [28, 36]. An industrial year is 8000 h, the MOT₈₀₀₀ is usually used to express the long-term stability of an ILs, and calculate MOT based on the experimental data obtained by [Bmim]BF₄ under two different atmospheres (Table 4). As shown in Fig. 6, based on DTG data for different heat rate

in dynamic thermogravimetric experiments, all curves have approximately the same slope (E_a/R) and a consistent $\ln A$; the long-term thermal stability of [Bmim]BF₄ can be calculated using Eq. (8) [29].

$$\ln\left(-\frac{dm}{dt}\right) = \ln(k_0) - \frac{E_a}{R} \times \frac{1}{T} + \ln(m) \quad (7)$$

$$\text{MOT} = \frac{E_a}{R \times [4.6 + \ln(A \times t_{\max})]} \quad (8)$$

Under nitrogen, the MOT for [Bmim]BF₄ is about 112 °C for 8000 h (MOT₈₀₀₀), but 185 °C for 24 h (MOT₂₄) and circa 238 °C for only 1 h of application (MOT₁). Under air, the MOT for [Bmim]BF₄ is about 92 °C for 8000 h, but 169 °C for 24 h and circa 225 °C for only 1 h of application. From Table 4, MOT decreases with the increase in usage time. When [Bmim]BF₄ is used for a long time, its temperature range should be strictly controlled to prevent danger. The value of MOT in air is less than that in nitrogen, which indicates that the risk of [Bmim]BF₄ in air is higher than that in nitrogen. Ultimately, these calculated values fit very well the observed decomposition behavior in short-term measurements of about 1 h for [Bmim]BF₄; thermal decomposition with mass loss of 1% or higher has been observed at temperatures above circa 200 °C.

Analysis of pyrolysis products by infrared spectroscopy

The reaction mechanism of [BMIM]BF₄ differs between air and nitrogen conditions, and the decomposition products are investigated using FTIR. As shown in Fig. 7a, there is only one product peak under nitrogen. The wave number range between 2879, 2965, and 2942 cm⁻¹ is the asymmetric and symmetric stretching vibration of C–H. The wave number range between 3152 and 3112 cm⁻¹ is the stretching vibration of C–H of unsaturated carbon. The wave numbers at 1569 are due to C=N stretching. The peak of wave numbers at 1465 cm⁻¹ is due to CH₃ and CH₂ asymmetric bending of alkyl substituent. Wave number of 1352 cm⁻¹ is the bending vibration of C–H, and wave number range of 1191 cm⁻¹ is the stretching vibration of C–F bond. The wave number range is 1140 cm⁻¹ for C–C bond stretching vibration and 1060 cm⁻¹ is due to stretching vibration of anion BF₄⁻. The band of 846 cm⁻¹ is due to C–N stretching vibrations.

There is only one product peak under air, as shown in Fig. 7b, the wave number range from 2900 is the stretching vibration of the C–H bond, and the wave number at 2359 cm⁻¹ is the asymmetric stretching vibration of the O=C=O bond in CO₂. The wave number at 1060 cm⁻¹ is due to stretching vibration of anion BF₄⁻. From the known functional groups, it can be initially determined

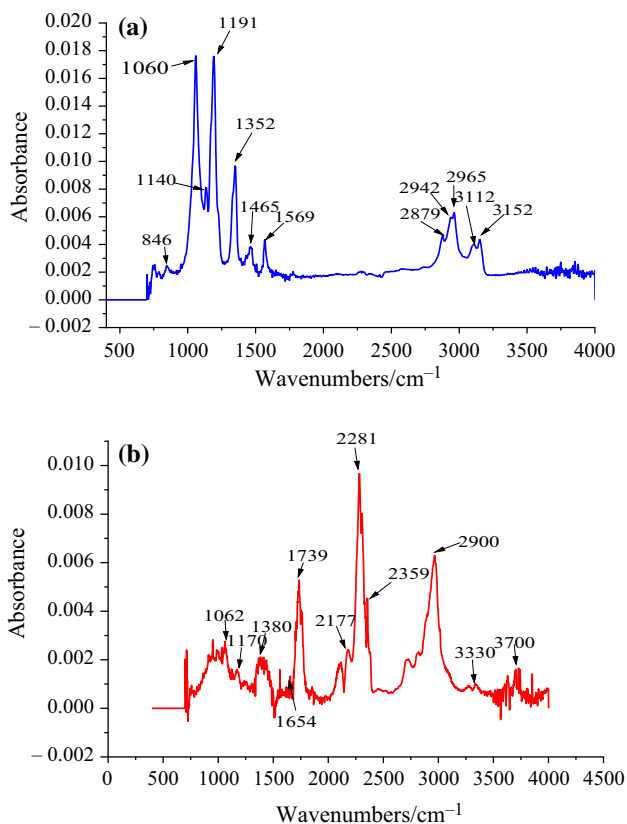


Fig. 7 Image **a** infrared spectra of meteorological decomposition products of [Bmim]BF₄ under nitrogen, image **b** infrared spectra of meteorological decomposition products under air

that the gaseous product contains methanol (C–H bond stretching vibration: 3000–2900 cm⁻¹, O–H stretching vibration: 3400–3230 cm⁻¹, C–O bond stretching vibration: 1062 cm⁻¹). Methyl isocyanate may also be present in the emission gas (O=C=N bond stretching vibration: 2281–2309 cm⁻¹, C–H stretching vibration: 3000–2900 cm⁻¹).

It can be found that the products in the two atmospheres are completely different, and combustion reactions occur under air conditions with oxidation products, thus giving off amount of heat. This indicates that ILs are not safe in air conditions and serious safety accidents may occur, so their thermal hazards in both air and nitrogen atmospheres are studied by ARC.

To prevent the drawback of analyzing the decomposition mechanism only by infrared spectrograms at peak product concentrations, the 3–D infrared transform spectra of [BMIM]BF₄ in air with nitrogen release gas are shown in Figs. 8 and 9.

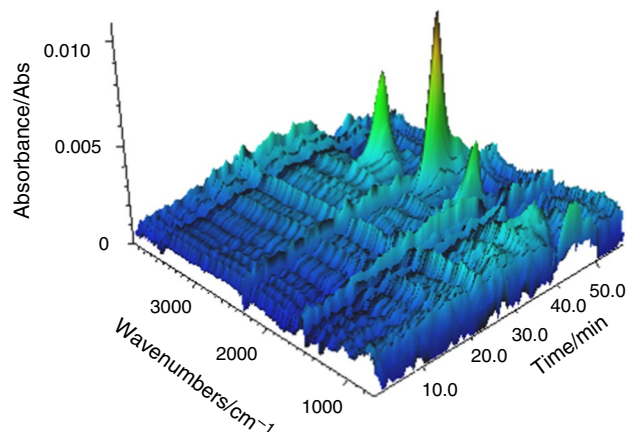


Fig. 8 3-D FTIR spectra of gases released from the decomposition of [Bmim]BF₄ under air atmosphere

Decomposition characteristics of ionic liquids under two atmospheres studied by ARC

As a desulfurizer of liquid fuel, thermal runaway of [BMIM]BF₄ will have a great influence on the use of liquid fuel and may cause fire or even explosion if the decomposition reaction is out of control in a confined space. In order to study whether air and nitrogen reduce their thermal hazards under adiabatic conditions, pressure rise rate, temperature rise rate, maximum pressure, and maximum temperature are used to quantitatively evaluate the thermal hazards [37]. ARC data on temperature and pressure versus time are shown in Figs. 10 and 11.

The exotherm of [Bmim]BF₄ is detected at 383.0 °C under air and reaches the maximum temperature rise rate under adiabatic conditions after 46 min. The maximum temperature and pressure rise rates are 1.2500 °C min⁻¹ and 0.8960 bar min⁻¹; the maximum pressure and maximum temperature reached are 73.9 bar and 451.7 °C, respectively. Similarly, exotherm was

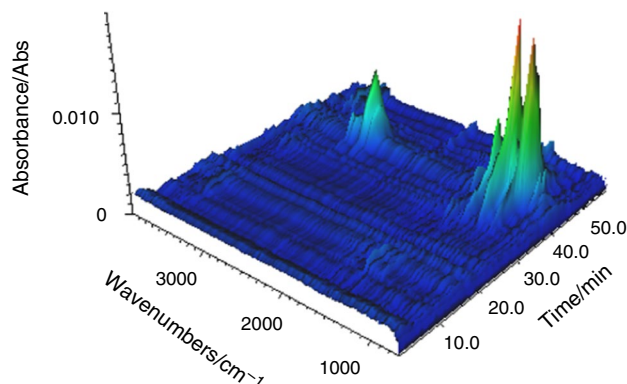


Fig. 9 3-D FTIR spectra of gases released from the decomposition of [Bmim]BF₄ under nitrogen atmosphere

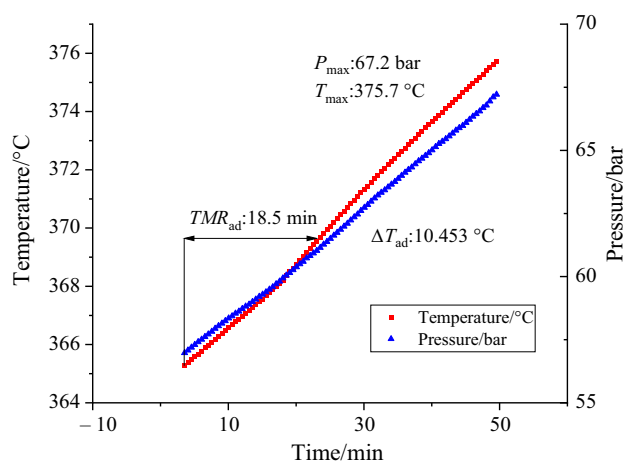


Fig. 10 Temperature and pressure versus time of [Bmim]BF₄ by ARC under nitrogen

detected at 365.0 °C under nitrogen and maximum temperature rise rate reached after 18.5 min, where maximum temperature rate and pressure rise rate are 0.2880 °C min⁻¹ and 0.2840 bar min⁻¹ and the maximum pressure and maximum temperature are 67.2 bar and 375.7 °C, respectively. Higher temperature and pressure under air conditions as a result of the exothermic combustion of its pyrolysis products and the production of CO₂, higher heating rate and pressure rise rate, reducing the reaction time, higher temperature, and pressure increase its destructive, indicating that the adiabatic runaway of [Bmim]BF₄ is more dangerous when it placed in air conditions. In order to further explain different hazards in the two atmospheres, the reaction mechanism needs to be investigated.

Dynamics under adiabatic conditions

The thermodynamic method in this paper under adiabatic conditions was proposed [37], for an n-order reaction with a single reactant; the self-heating reaction is expressed as follows [38, 39]:

$$m_T = \frac{dT}{dt} = \Delta T_{ad} \left[\frac{T_f - T}{T_f - T_0} \right]^n K \quad (9)$$

m_T is the self-heating rate at any temperature, n is the reaction order, T_0 and T_f are the starting and ending temperatures, respectively, ΔT_{ad} is the adiabatic temperature rise, and K is the rate constant. K can be expressed as follows:

$$K = \frac{m_T}{\Delta T_{ad} \left[\frac{T_f - T}{\Delta T_{ad}} \right]^n} \quad (10)$$

Based on the Arrhenius equation, we can find E_a and A by the following formula.

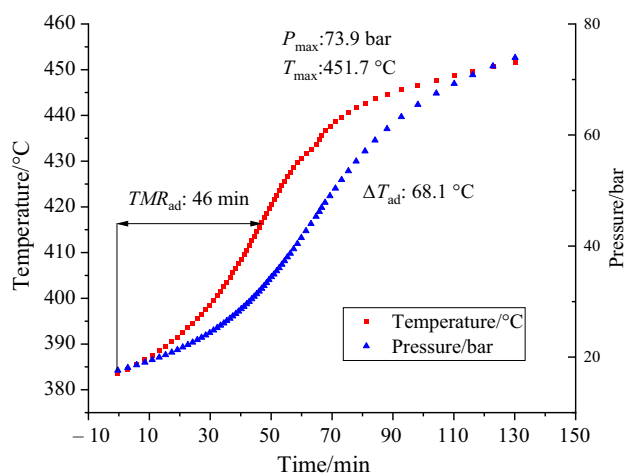


Fig. 11 Temperature and pressure versus time of [Bmim]BF₄ by ARC under air

$$\ln k = -\frac{E_a}{R} \times \frac{1}{T} + \ln A \quad (11)$$

Thermal inertia correction of thermal decomposition parameters under adiabatic conditions

Under ideal adiabatic conditions, the adiabatic temperature rise is provided by the heat released from the decomposition reaction. But there is the fact situation the heat generated by the decomposition reaction is not only used to raise the temperature, but also partly absorbed by the calorimeter, so this experiment needs to be corrected by using the thermal inertia factor [40, 41].

$$\varphi = 1 + \frac{M_c C_{vc}}{M_s C_{vs}} \quad (12)$$

where M_c is the mass of the test bomb of ARC, M_s is the mass of the sample. C_{vc} is the heat capacity of the bomb, C_{vs} is the heat capacity of the sample.

The temperature correction equation is as follows:

$$T'_{end} = T_{star} + \varphi(T_{end} - T_{star}) \quad (13)$$

The correction for the adiabatic temperature rise is as follows:

$$\Delta T'_{ad} = \varphi \Delta T_{ad} \quad (14)$$

Using the thermal inertia parameter to correct the experimental data and making Figs. 12 and 13, the gas atmosphere affects the decomposition mechanism of [Bmim]BF₄, the pyrolysis reaction in air is third-order

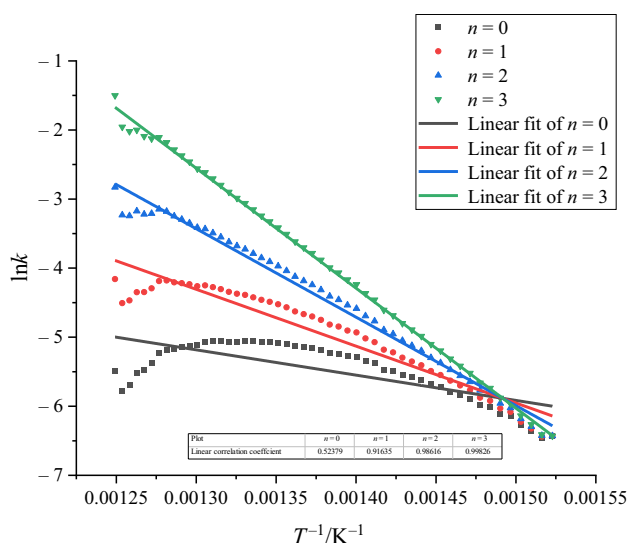


Fig. 12 Linear fit for $\ln k$ to T^{-1} curve with different reaction orders under air

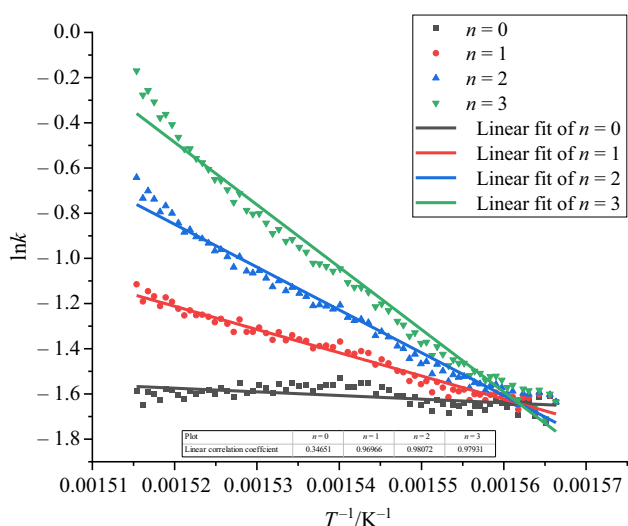


Fig. 13 Linear fit for $\ln k$ to T^{-1} curve with different reaction orders under nitrogen

reaction, and under nitrogen it is second-order reaction. As shown in Figs. 10 and 11, the starting pressure under nitrogen is 57 bar much higher than that under air 15 bar; the difference reaction order between the two atmospheres causes difference in the reaction mechanism. As shown in Fig. 14, the self-heating rate varies with time, the maximum self-heating rate is reached faster under nitrogen, but the value of self-heating rate under nitrogen is much smaller than that under air due to the suppress effect of nitrogen. Nitrogen will make it decompose earlier, but nitrogen will suppress the thermal effect, even if the decomposition is earlier, but the degree of harm that be

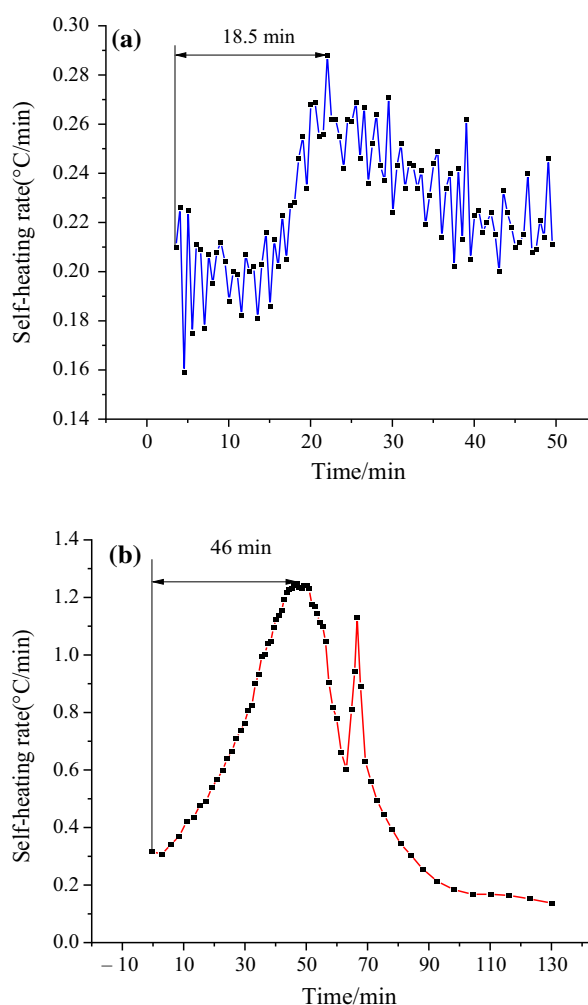


Fig. 14 Image a the self-heating rate varies with time under nitrogen; image b the self-heating rate varies with time under air

achieved is limited and less than that caused by the combustion of the product in air.

Conclusions

In this study, [Bmim]BF₄ proved to be potentially dangerous, contrary to traditional defined. From thermogravimetric experiments, it can be find that the onset temperature of all heating rates under air conditions [Bmim]BF₄ is significantly lower than the onset temperature of all temperature rates under nitrogen conditions, and the E_a under air condition is lower than that under nitrogen condition. By calculating the long-term thermal stability of [Bmim]BF₄, MOT₈₀₀₀ is 92 °C under air conditions and 112 °C under nitrogen conditions, which proves that the long-term thermal stability of [Bmim]BF₄ under air conditions is lower than that under nitrogen conditions. This indicates that [Bmim]BF₄ is more

unstable under air conditions. By TG-FTIR experiments, it was demonstrated that the pyrolysis products of [Bmim]BF₄ in the two atmospheres are different; the products under air conditions burn and produce carbon dioxide and release heat, which explains the great exotherm produced in the DSC images under oxygen conditions. By ARC, it is found that the thermal effect of [Bmim]BF₄ under nitrogen conditions is limited, and the thermal effect under air conditions is quite obvious. By fitting the adiabatic data, the reaction orders under different atmospheres were obtained, indicating the different in the reaction mechanism of [Bmim]BF₄ under air and nitrogen conditions.

A comprehensive analysis of the thermal stability and decomposition mechanism of [Bmim]BF₄ under air and nitrogen conditions shows that ILs are not as safe as traditionally thought. For the long-term storage, [Bmim]BF₄ should be avoided as much as possible under air condition. Without considering the cost, the flowing inert gas atmosphere plays a certain role in ensuring the safety of [Bmim]BF₄.

Acknowledgements This work was supported by the National Natural Science Foundation of China (52104177) and the Independent Research fund of Key Laboratory of Industrial Dust Prevention and Control & Occupational Health and Safety, Ministry of Education (Anhui University of Science and Technology) (NO. EK20211006)

References

- Rogers RD, Seddon KR. Ionic liquids—solvents of the future? *Science* (1979). *Am Assoc Adv Sci*. 2003;302:792–3.
- Fang DW, Liang KH, Hu XH, Fan XT, Wei J. Low-temperature heat capacity and standard thermodynamic functions of 1-hexyl-3-methyl imidazolium perchlorate ionic liquid. *J Therm Anal Calorim*. 2019;138:1641–7.
- Dong K, Liu X, Dong H, Zhang X, Zhang S. Multiscale studies on ionic liquids. *Chem Rev*. 2017;117:6636–95.
- Mu T, Han B. Structures and thermodynamic properties of ionic liquids. *Struct Interact Ion Liq*. 2014;151:107–39.
- Bakkar A, Neubert V. Electrodeposition and corrosion characterization of micro- and nano-crystalline aluminium from AlCl₃/1-ethyl-3-methylimidazolium chloride ionic liquid. *Electrochim Acta*. 2013;103:211–8.
- Schneider S, Hawkins T, Ahmed Y, Deplazes S, Mills J. Ionic liquid fuels for chemical propulsion. *Ionic Liquids Sci Appl*. ACS Publications; 2012;1117:1–25.
- Tsai CF, Wen JJ. Reaction mode on the green construction process and corresponding thermal stability evaluation of ionic liquid. *J Therm Anal Calorim*. 2022;147:10745–54. <https://doi.org/10.1007/s10973-022-11314-7>
- Liu S-H, Zhang B, Cao C-R. Evaluation of thermal properties and process hazard of three ionic liquids through thermodynamic calculations and equilibrium methods. *J Loss Prev Process Ind*. 2020;68:104332.
- Chen C-C, Liaw H-J, Chen Y-N. Flammability characteristics of ionic liquid 1-Decyl-3-methylimidazolium bis (trifluoromethylsulfonyl) imide. *J Loss Prev Process Ind*. 2017;49:620–9.
- Parajó JJ, Teijeira T, Fernández J, Salgado J, Villanueva M. Thermal stability of some imidazolium [NTf₂] ionic liquids: Isothermal and dynamic kinetic study through thermogravimetric procedures. *J Chem Thermodyn*. 2017;112:105–13.
- Ohtani H, Ishimura S, Kumai M. Thermal decomposition behaviors of imidazolium-type ionic liquids studied by pyrolysis-gas chromatography. *Anal Sci*. 2008;24:1335–40.
- Wasserscheid P, Welton T. *Ionic liquids in synthesis*. New York: Wiley; 2008.
- del Sesto RE, McCleskey TM, Macomber C, Ott KC, Koppisch AT, Baker GA, et al. Limited thermal stability of imidazolium and pyrrolidinium ionic liquids. *Thermochim Acta*. 2009;491:118–20.
- Baranyai KJ, Deacon GB, MacFarlane DR, Pringle JM, Scott JL. Thermal degradation of ionic liquids at elevated temperatures. *Aust J Chem*. 2004;57:145–7.
- Fox DM, Gilman JW, de Long HC, Trulove PC. TGA decomposition kinetics of 1-butyl-2, 3-dimethylimidazolium tetrafluoroborate and the thermal effects of contaminants. *J Chem Thermodyn*. 2005;37:900–5.
- Wooster TJ, Johanson KM, Fraser KJ, MacFarlane DR, Scott JL. Thermal degradation of cyano containing ionic liquids. *Green Chem*. 2006;8:691–6.
- Dharaskar SA, Wasewar KL, Varma MN, Shende DZ, Yoo C. Synthesis, characterization and application of 1-butyl-3-methylimidazolium tetrafluoroborate for extractive desulfurization of liquid fuel. *Arabian J Chem*. 2016;9:578–87.
- Gerbaud V, Rodriguez-Donis I, Hegely L, Lang P, Denes F, You X. Review of extractive distillation. *Process design, operation, optimization and control*. *Chem Eng Res Des*. 2019;141:229–71.
- Wang W-T, Liu S-H, Wang Y, Yu C-F, Cheng Y-F, Shu C-M. Thermal stability and exothermic behaviour of imidazole ionic liquids with different anion types under oxidising and inert atmospheres. *J Mol Liq*. 2021;343:117691.
- Huang A-C, Li Z-P, Liu Y-C, Tang Y, Huang C-F, Shu C-M, et al. Essential hazard and process safety assessment of para-toluene sulfonic acid through calorimetry and advanced thermokinetics. *J Loss Prev Process Ind*. 2021;72:104558.
- Zhou H-L, Jiang J-C, Huang A-C, Tang Y, Zhang Y, Huang C-F, et al. Calorimetric evaluation of thermal stability and runaway hazard based on thermokinetic parameters of O, O-dimethyl phosphoramidothioate. *J Loss Prev Process Ind*. 2022;75:104697.
- Yang N, Jiang JC, Huang AC, Tang Y, Li ZP, Cui JW, et al. Thermokinetic model-based experimental and numerical investigation of the thermal hazards of nitrification waste. *J Loss Prev Process Ind*. 2022;79:104836.
- Wu H, Jiang JC, Huang AC, Tang Y, Liu YC, Zhai J, et al. Effect of emulsifiers on the thermal stability of firework propellants. *J Therm Anal Calorim*. 2022. <https://doi.org/10.1007/s10973-022-11473-7>
- Liu S-H, Guo R-L, Li F-H, Chiang C-L. Thermal analysis and pyrolysis products analysis of 4,4'-azobis (4-cyanovaleric acid) by using thermal analysis methods and combination technology. *J Therm Anal Calorim*. 2022. <https://doi.org/10.1007/s10973-022-11571-6>
- Wang Y, Liu S-H, Chiang C-L, Zhang L-Y, Wang W-T. The effect of oxygen on the thermal stability and decomposition behaviours of 1, 3-dimethylimidazolium nitrate for application using STA, ARC and FTIR. *Process Safety Environ Protect*. 2022;162:513–9.
- Wang Y-R, Liu J-P, Chen L-P, Shao X-Y, Xu S. Thermal decomposition characteristics and runaway boundary conditions of HATO at adiabatic and high pressure situations. *Process Safety and Environmental Protection [Internet]*. 2022. <https://linkinghub.elsevier.com/retrieve/pii/S0957582022008187>
- Wu H-B, Zhang B, Liu S-H, Chen C-C. Flammability estimation of 1-hexyl-3-methylimidazolium bis (trifluoromethylsulfonyl) imide. *J Loss Prev Process Ind*. 2020;66:104196.

28. Efimova A, Pfützner L, Schmidt P. Thermal stability and decomposition mechanism of 1-ethyl-3-methylimidazolium halides. *Thermochim Acta*. 2015;604:129–36.
29. Zhang B, Liu S-H, Liu J, Zhang Z-H, Laiwang B, Shu C-M. Thermal stability and flammability assessment of 1-ethyl-2,3-dimethylimidazolium nitrate. *Process Safety Environ Protect*. 2020;135:219–27.
30. Huang AC, Huang CF, Tang Y, Xing ZX, Jiang JC. Evaluation of multiple reactions in dilute benzoyl peroxide concentrations with additives using calorimetric technology. *J Loss Prev Process Ind*. 2021;69:104373.
31. Vyazovkin S, Burnham AK, Criado JM, Pérez-Maqueda LA, Popescu C, Sbirrazzuoli N. ICTAC Kinetics Committee recommendations for performing kinetic computations on thermal analysis data. *Thermochim Acta*. 2011;520:1–19.
32. Huang AC, Liao FC, Huang CF, Tang Y, Zhang Y, Shu CM, et al. Calorimetric approach to establishing thermokinetics for cosmetic benzoyl peroxides containing metal ions. *J Therm Anal Calorim*. 2021;144:373–82.
33. Li ZP, Huang AC, Tang Y, Zhou HL, Liu YC, Huang CF, et al. Thermokinetic prediction and safety evaluation for toluene sulfonation process and product using calorimetric technology. *J Therm Anal Calorim*. 2022;147:12177–86. <https://doi.org/10.1007/s10973-022-11384-7>
34. Lu G, Yang T, Chen L, Zhou Y, Chen W. Thermal decomposition kinetics of 2-ethylhexyl nitrate under non-isothermal and isothermal conditions. *J Therm Anal Calorim*. 2016;124:471–8.
35. Vyazovkin S, Burnham AK, Criado JM, Pérez-Maqueda LA, Popescu C, Sbirrazzuoli N. ICTAC Kinetics Committee recommendations for performing kinetic computations on thermal analysis data. *Thermochim Acta*. 2011;520:1–19.
36. Seeberger A, Andresen A-K, Jess A. Prediction of long-term stability of ionic liquids at elevated temperatures by means of non-isothermal thermogravimetric analysis. *Phys Chem Chem Phys*. 2009;11:9375–81.
37. Lu Y-M, Liu S-H, Shu C-M. Evaluation of thermal hazards based on thermokinetic parameters of 2-(1-cyano-1-methylethyl) azocarboxamide by ARC and DSC. *J Therm Anal Calorim*. 2019;138:2873–81.
38. Guo RL, Liu SH, Shu CM. Thermal hazard evaluation conjoined with product analysis of two water-soluble azo compounds. *J Therm Anal Calorim*. 2022;147:10775–84. <https://doi.org/10.1007/s10973-022-11257-z>
39. Wang YR, Liu SH, Cheng YC. Thermal analysis and hazards evaluation for HTP-65W through calorimetric technologies and simulation. *J Therm Anal Calorim*. 2021;144:1483–92.
40. Hua M, Wei C, Guo X, Liang X, Pan X, Yu A, et al. Thermal hazard evaluation of tert-butylperoxy-2-ethylhexanoate mixed with H₂O and NaOH solution. *Chem Eng Commun*. 2020;207:1636–45.
41. Liu Y-C, Jiang J-C, Huang A-C, Tang Y, Yang Y-P, Zhou H-L, et al. Hazard assessment of the thermal stability of nitrification by-products by using an advanced kinetic model. *Process Safety Environ Protect*. 2022;160:91–101.

Publisher's Note Springer Nature remains neutral with regard to jurisdictional claims in published maps and institutional affiliations.

Springer Nature or its licensor (e.g. a society or other partner) holds exclusive rights to this article under a publishing agreement with the author(s) or other rightsholder(s); author self-archiving of the accepted manuscript version of this article is solely governed by the terms of such publishing agreement and applicable law.